

LIGHT INTENSITY DISTRIBUTION IN PHOTOCATALYTIC REACTORS USING A FINITE VOLUME METHOD

Vishnu K. PAREEK¹, Shane COX² and Adesoji A. ADESINA^{2*}

¹Department of Chemical Engineering, Curtin University of Technology, GPO Box U1987 Perth, WA, 6845, Australia

²Reactor Engineering and Technology Group, School of Chemical Engineering and Industrial Chemistry, University of New South Wales, NSW, 2052, Australia

ABSTRACT

A conservative variant of discrete ordinate model was used to solve the radiation transport equation. The model prediction was used to assess the effect of wall reflectivity, catalyst loading and phase function parameter on the light intensity distribution in an annular heterogeneous photocatalytic reactor. For relatively low catalyst loadings, the wall reflectivity strongly influenced the light intensity distribution. However, for an optically thick medium, the wall reflectivity had very little or no effect. The volume-average light intensity distribution decreased rather sharply with the catalyst loading and opposite trend was obtained for the local volumetric rate of energy absorption (LVREA). However, after the initial sharp increase, the LVREA appeared independent of catalyst loading.

NOMENCLATURE

e	=	emissivity
E_{bg}	=	band gap energy, J
E_l	=	local volumetric rate of energy absorption, einstein $m^{-3} s^{-1}$
G	=	total incident radiation, einstein $m^{-2} s^{-1}$
I	=	radiation intensity, einstein $m^{-2} s^{-1} sr^{-1}$
K_l	=	total lamp specific emission parameter, einstein $m^{-1} s^{-1}$
L	=	semi-length of lamp, m, and also total number control volumes, dimensionless
$p(\Omega \rightarrow \Omega')$	=	phase function for scattering in RTE, dimensionless
r_{ref}	=	reflectivity
R	=	radius of lamp-cooling assembly, m
t	=	transmittivity
W_{cat}	=	catalyst loading, $g m^{-3}$
x, y, z	=	Cartesian coordinate, m
<i>Greek</i>		
Ω	=	solid angle, steradian
σ	=	scattering coefficient, m^{-1}
κ	=	absorption coefficient, m^{-1}
λ	=	wavelength of radiation, m
ν	=	frequency of radiation, s^{-1}
$\mu^l \xi^l \eta^l$	=	direction cosines

Subscripts

ν = frequency of radiation

Superscripts

l = l^{th} control angle

Acronyms

DO = discrete ordinate

FV = finite volume

LVREA = local volumetric rate of energy absorption, einstein $m^{-3} s^{-1}$

RTE = radiation transport equation

INTRODUCTION

The involvement of radiation is the single most important factor that distinguishes the photochemical/photocatalytic reactor from the conventional thermally activated reactive processes. The rate of initiation (in case of photocatalysis, electron-hole formation) step in photochemical reaction is directly dependent on the radiation intensity (Cassano et al. 1995). Since the step of electron-hole formation is a fast one (time constant $\approx 10^{15} s^{-1}$), in a well illuminated reactor, it may be expected that light intensity will not be a rate determining step. However, it is highly difficult to maintain a uniform light intensity within a reactor space and the intensity distribution invariably determining the overall conversion and reactor performance. The radiation transport equation (RTE) that describes the light intensity distribution is an integro-differential equation, and an exact analytical solution is possible only for highly ideal one-dimensional situations (Carvalho and Farias 1998). For photocatalytic reactors, however, due to light scattering in the presence of titania particles, it is impossible to find an analytical solution for the RTE.

The light intensity distribution in a photoreactor is determined by a number of factors, namely, (i) the lamp type, (ii) the lamp-reactor geometry, (iii) the optical properties of medium, and (iv) the nature of reactor walls. In this paper, we investigate the light intensity distribution in a 14-L pilot scale annular photoreactor previously described (Pareek et al. 2001) with special emphasis on the effect of reactor wall reflectivity. The parameters of the lamp used in this study are reported in Table 1.

*Corresponding author, Email: a.adesina@unsw.edu.au, Fax: +61-2-9385-5661

Type	Parameter	Value
Medium-pressure mercury lamp (Primac, AVP06C)	Diameter (D_{lamp})	2.0 cm
	Length (L_{lamp})	15.0 cm
	Average UV production efficiency (between 290-400 nm)	22–25 %
	Total emission (at 300 W)	10^{-4} einstein s^{-1}

Table 1. Lamp parameters.

MODEL DEVELOPMENT

Radiation Transport Equation

The formulation of radiation transport equation (RTE) is well established and has been widely used in the furnace design application and solar radiation characterization for a fairly long time (Chandrasekhar 1960). Application of the RTE to photocatalytic processes is, however, recent (Cassano et al. 1995; Spadoni et al. 1978). After making a radiation balance across a thin slab and substituting appropriate constitutive relations (Cassano et al. 1995; Pareek and Adesina 2003b), the RTE may be expressed as:

$$\frac{dI_v(s, \Omega)}{ds} = -\kappa_v I_v(s, \Omega) - \sigma_v I_v(s, \Omega) + \frac{1}{4\pi} \sigma_v \int_{4\pi} p(\Omega' \rightarrow \Omega) I_v(s, \Omega') d\Omega' \quad (1)$$

where, the first term on the right hand side represents the loss of photons due to absorption, the loss of radiation due to out-scattering is accounted for in the second term, and the last term accounts for the gain in the radiation due to in-scattering; $p(\Omega' \rightarrow \Omega)$ is the phase function for the in-scattering of photons.

The incident intensity at any point from all the directions is given by:

$$G_v(s) = \int_{\Omega=0}^{\Omega=4\pi} I_v(s, \Omega) d\Omega \quad (2)$$

The local volumetric rate of energy absorption (LVREA) at any point is given by:

$$E_{l,v}(s) = \kappa_v G_v(s) \quad (3)$$

For photocatalytic applications, only those photons with a wavelength less than or equal to the band gap energy $\lambda_{E_{bg}}$ contribute to the excitation of electrons in the semiconductor particles. A summation may be carried out over this wavelength range to evaluate the total LVREA:

$$E_l = \sum_{\lambda < \lambda_{E_{bg}}} E_{l,v}(s) = \sum_{\lambda < \lambda_{E_{bg}}} \kappa_v G_v(s) \quad (4)$$

Optical Properties of Reactive Medium

Optical properties of the reaction medium play an important role in the overall design of a photoreactor. For example, in homogeneous photochemical reactors, the size of reactor vessel for a given conversion increases exponentially with the optical thickness (defined as $\kappa \times$ distance). In homogeneous systems, only one parameter – the absorption coefficient (κ) – is involved, which may be readily estimated using the Beer-Lambert law. However, for heterogeneous systems, the RTE described

in the previous section contains three parameters, namely, the absorption coefficient (κ), the scattering coefficient (σ) and the phase function (p).

Absorption and Scattering Coefficients

Values of κ and σ for titania catalyst depend on the wavelength of the light. Therefore, the RTE should be solved for the each of the individual wavelength ranges. However, this will make the computations memory-intensive. Consequently, in this study, we have used the wavelength-averaged values of the absorption and scattering coefficients (Romero et al. 1997):

$$\sigma = 3.598 \times W_{cat} \quad (5)$$

$$\kappa = 0.2758 \times W_{cat} \quad (6)$$

where σ and κ are the wavelength-averaged scattering and absorption coefficients (m^{-1}) and W_{cat} is the catalyst loading ($g\ m^{-3}$).

Phase Function Parameter

For the isotropic scattering, the phase function parameter has a value, unity. However, for anisotropic scattering, a number of expressions have been reported and each one of them is suitable for specific systems. The widely used phase function is of linear anisotropic form (Fiveland 1984):

$$p(\theta) = 1 + a_o \cos(\theta) \quad (7)$$

with $a_o = 1, 0, -1$ for forward, isotropic and backward scattering respectively. In terms of direction cosines, the phase function may be expressed as:

$$p(\Omega^m \rightarrow \Omega^l) = 1 + a_o (\mu^l \mu^m + \xi^l \xi^m + \eta^l \eta^m) \quad (8)$$

where μ^l, ξ^l and η^l are the direction cosines of l^{th} direction and μ^m, ξ^m and η^m are the direction cosines of m^{th} direction.

RESULTS AND DISCUSSION

To illustrate the utilisation of FV method for estimating the light intensity in a photoreactor, FLUENT 6.0 solver was used to numerically solve the RTE in a pilot scale photoreactor (Pareek et al. 2001). The characteristics of the lamp used in this study are listed in Table 1. The simulations were performed for different catalyst loadings and reactor wall reflectivities. The volume-averaged values of scattering and absorption coefficients for titania particles were obtained using equations (5) and (6) (Romero et al. 1997).

Physical Picture and Solution Domain

The computational domain of the annular pilot-scale photoreactor (OD = 20 cm, ID = 8 cm length = 120 cm,

lamp length = 15 cm, lamp OD = 2 cm) used in this study is shown in Figure 1(a). The reaction mixture flows in the annular space. The centrally placed UV lamp is cooled by the running water to maintain a uniform reaction-temperature as well as to remove IR fraction of the UV lamp. The UV absorption takes place mainly in the annular reaction-space and the absorption within the cooling section is negligible. Therefore, in this analysis, we have discarded the central lamp assembly from a mathematical consideration; instead the light intensity (or incident radiation) at the inner wall was determined using a line source model (equation (14)).

The axi-symmetric nature of the present reactor geometry with respect to radiation distribution allowed a 2D computational geometry. Furthermore, the mirror symmetry permitted the calculations only in the one half and the other half could be taken as resolved. Figure 1(b) shows the final geometry meshed with 861 quadrangle grids. The water inlet and outlet made no contribution in the radiation intensity and were, therefore, discarded in order to improve the computational efficiencies.

Boundary Conditions

When a certain amount of radiation is incident on a wall, a part of it may be absorbed; a part of it may be transmitted; and the remaining may be reflected. Therefore, following relation holds for a wall:

$$a + t + r_{ref} = 1 \quad (9)$$

where, a is the absorptivity of the wall, t is its transmittivity and r_{ref} is the reflectivity. For a blackbody wall, Kirchoff's principle is applicable:

$$a = e \quad (10)$$

where, e is the emissivity of the walls. Using equation (10) in equation (9), we have:

$$e + t + r_{ref} = 1 \quad (11)$$

Since in the current reactor configuration, the reactor walls were non-transparent, $t = 0$, equation (11) reduces to:

$$e + r_{ref} = 1 \quad (12)$$

As FLUENT solver accepts values only for the emissivity, for a desired reflectivity r_{ref} , e values should be calculated using equation (12).

For setting up the boundary conditions, following assumptions were made:

1. Rate of emission of radiation per unit area from the lamp surface is constant.
2. The reactor-surfaces are non-emitting but may be reflecting diffusely or specularly.

Consequently, the boundary conditions may be summarised as follows:

Inner Surface

The incident radiation heat flux is given by:

$$G_{in}^{inner} = \int_{\mathbf{s} \cdot \mathbf{n} > 1, inner_surface} I_{in} \mathbf{s} \cdot \hat{\mathbf{n}} d\Omega \quad (13)$$

where, \mathbf{s} is the direction of the incident radiation, $\hat{\mathbf{n}}$ is a unit vector normal to plane of incidence and Ω is the solid angle.

The net radiative flux leaving the surface is given by:

$$G_{out}^{inner} = r_{ref}^{inner} G_{in}^{inner} + \frac{K_1}{4\pi R} \left(\tan^{-1} \left(\frac{x+L}{R} \right) - \tan^{-1} \left(\frac{x-L}{R} \right) \right) \quad (14)$$

where, r_{ref}^{inner} is the reflectivity of the inner surface, K_1 is radiant power per unit length of the lamp (einstein $\text{m}^{-1} \text{s}^{-1}$), x denotes axial coordinate, R is the radius of the cooling assembly (4 cm in Figure 1(a)) and L is the semi-length of the lamp. A *user defined function* was used to accommodate equation (14) in the FLUENT solver.

In a 2D space, the out-going intensity in all the directions at the lamp surface is calculated by dividing the incident radiation with π (the total of all outgoing directions):

$$I_{out}^{inner} = \frac{G_{out}^{inner}}{\pi} \quad (15)$$

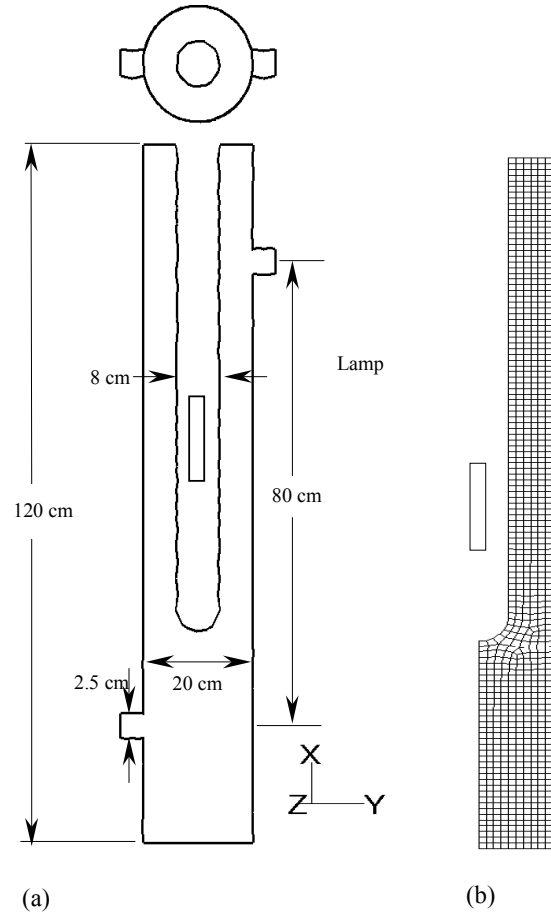


Figure 1. (a) Geometry of the pilot-scale reactor. (b) 2D grids used in finite volume radiation calculations.

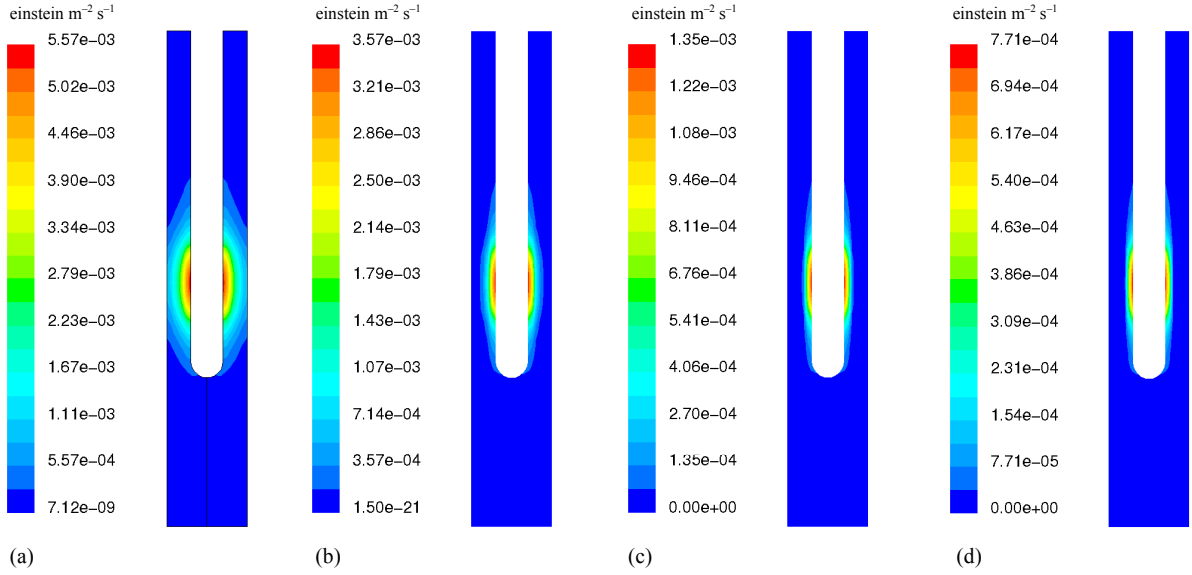


Figure 2. Contours of incident radiation with high optical density. (a) Diattinic medium ($\kappa = \sigma = 0 \text{ m}^{-1}$), (b) $W_{\text{cat}} = 0.10 \text{ g L}^{-1}$ ($\kappa = 28 \text{ m}^{-1}$, $\sigma = 360 \text{ m}^{-1}$). (c) $W_{\text{cat}} = 0.50 \text{ g L}^{-1}$ ($\kappa = 140 \text{ m}^{-1}$, $\sigma = 1800 \text{ m}^{-1}$). (d) $W_{\text{cat}} = 1.0 \text{ g L}^{-1}$ ($\kappa = 280 \text{ m}^{-1}$, $\sigma = 3600 \text{ m}^{-1}$).

Outer Reactor Walls

The incident intensity at the outer wall is calculated as in equation (13):

$$G_{in}^{reactor} = \int_{\mathbf{s} \cdot \mathbf{n} > 1, reactor_surface} I_{in} \mathbf{s} \cdot \mathbf{n} d\Omega \quad (16)$$

The out-going intensity will depend on the reflective properties of the reactor walls. For *diffusely reflecting reactor walls*:

$$G_{out}^{reactor} = r_{ref}^{reactor} G_{in}^{reactor} \quad (17)$$

and

$$I_{out}^{reactor} = \frac{G_{out}^{reactor}}{\pi} \quad (18)$$

For *specularly reflecting reactor walls*, the intensity incident from a direction \mathbf{s} is reflected in a direction \mathbf{s}_r :

$$I_{out}^{reactor}(\mathbf{s}_r) = I_{in}^{reactor}(\mathbf{s}) \quad (19)$$

where, the directions \mathbf{s} and \mathbf{s}_r are related to each other according to Snell's law:

$$\mathbf{s}_r = \mathbf{s} - 2(\mathbf{s} \cdot \hat{\mathbf{n}})\hat{\mathbf{n}} \quad (20)$$

Solver Parameters

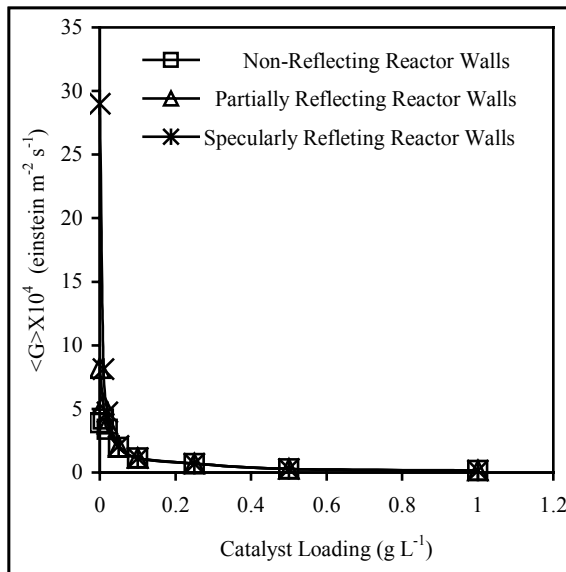
FLUENT's segregated solver was used to perform the numerical experiments. As in other finite volume calculations, the spatial discretization for the RTE is directly taken from the grid topology. However, the directional discretization for the RTE is supplied to the solver as a user-input. In the present study, because of axisymmetric nature a relatively smaller directional discretization was used. One quadrant of the grid space was divided into 8-discrete directions (total 32 directions). To avoid control angle overhang, a pixelation of 2×2 was

used throughout. A relaxation factor of unity was used to achieve the faster convergence. The calculations (iterations) were performed until the intensity residuals were less than or equal to 10^{-6} . A typical convergence history required about 100–200 iterations. This convergence was dependent on the values of optical parameters (κ and σ).

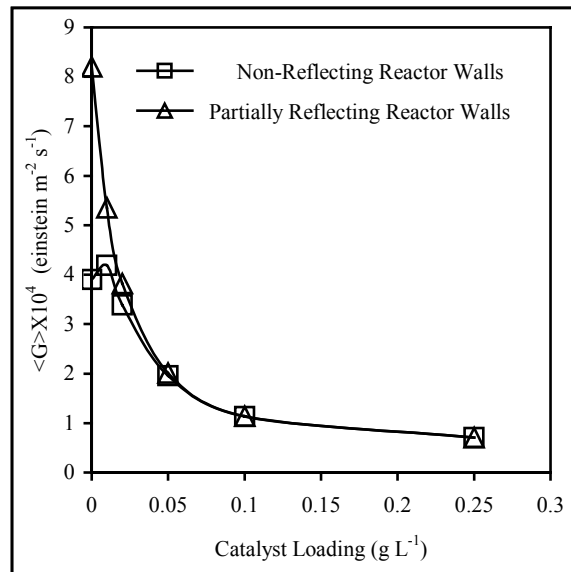
Effect of Catalyst Loading

Figure 2 shows contours of light intensity for four different catalyst loadings. For low catalyst loadings in Figure 2(a), the light intensity within the region of lamp length was nearly uniform. However, incident intensity dropped rather sharply beyond this region. Increase in catalyst loading resulted in decreased overall incident intensity. It is clear from Figure 2(b) that for $W_{\text{cat}} = 0.1 \text{ g L}^{-1}$, the illuminated zone was essentially confined to a narrow strip close to the glass assembly and most of the reactor space was rendered as dark. As may be apparent in Figure 2(c), when the catalyst loading was increased to 0.5 g L^{-1} , the illuminated strip was narrowed even further, eventually to turn to a thin line in Figure 2(d) for a catalyst loading 1.0 g L^{-1} . It is clear from the radiation profiles in Figures 2 that even for the radial points within the lamp zone the radiation intensities were zero just after 2-cm ($y \geq 0.06 \text{ m}$) from the lamp assembly. Therefore, it may be concluded that for the typical catalyst loadings (1.0 – 2.0 g L^{-1}) used in the photocatalytic applications, use of annular thickness ($r_o - r_i$) more than about 2-cm may not be useful. Cassano and coworkers (Cassano and Alfano 2000) made similar conclusions for a flat plate photoreactor.

Figure 3(a) shows effect of catalyst loading on volume-averaged incident radiation. Clearly, in the absence of photocatalyst, the specular walls gave a very high value of $\langle G \rangle$ ($\approx 3 \times 10^{-3} \text{ einstein m}^{-2} \text{ s}^{-1}$). However, with the introduction of catalyst particles, volume-average intensity dropped rather abruptly. After the catalyst loading of 0.02 g L^{-1} , different curves merged with each other and no meaningful observations could be made for the other two

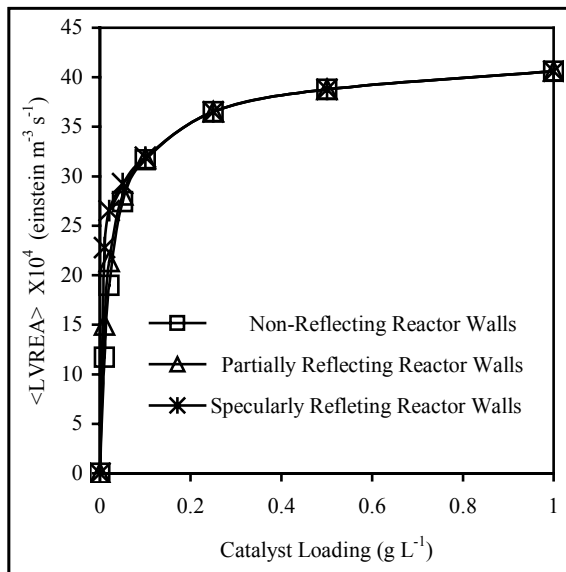


(a)

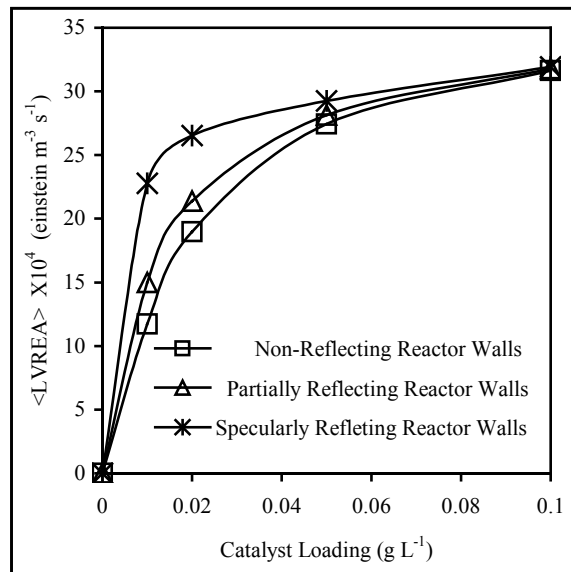


(b)

Figure 3. Effect of catalyst loading on the volume averaged incident radiation (with isotropic phase function) (a) Complete range. (b) On a more sensitive scale.



(a)



(b)

Figure 4. Effect of catalyst loading on the volume averaged LVREA (using isotropic phase function). (a) With complete range. (b) On a more sensitive scale.

wall reflectivities (non-reflecting and partially reflecting). Therefore, the behaviours shown by these two cases were redrawn in Figure 3(b) on a more sensitive x - y scale. The volume-averaged intensity for the partially reflecting reactor walls decreased sharply with the catalyst loading. Interestingly, the volume-averaged intensity for the non-reflecting reactor walls showed a minor increase initially and a maximum was obtained at 0.01 g L^{-1} . However, beyond this point, the intensity decreased quite progressively and eventually for $W_{cat} \geq 0.05 \text{ g L}^{-1}$, the two curves in Figure 3(b) merged.

Information on light intensity distribution was then used to calculate the volume-averaged local volumetric rate of energy absorption (LVREA) using equations (3) and (4). Figure 4(a) plots the volume averaged LVREA against the catalyst loading for the three different types of reactor walls. Initially, $\langle LVREA \rangle$ increased with the catalyst loading with the specularly reflecting reactor walls giving relatively higher values of $\langle LVREA \rangle$. However, after $W_{cat} = 0.050 \text{ g L}^{-1}$ the three curves in Figure 4(a) merged with each other and $\langle LVREA \rangle$ became constant irrespective of catalyst loading. Therefore, from the radiation absorption

point of view, the catalyst concentrations higher than this ($W_{cat} = 0.50 \text{ g L}^{-1}$) should not be important. In reality, however, the catalyst loadings greater than 2 g L^{-1} have been found to yield optimum results (Cassano and Alfano 2000). This is because the optimum catalyst loading is not determined solely by the optical properties of the reacting medium. Electrochemical factors such as pH and ionic strength may cause agglomeration and possibly change the optical characteristics of the medium itself. Furthermore, properties inherent to catalytic activity other than the photo absorption rates have strong influence on the reaction rates (Cassano and Alfano 2000). Therefore, it is not possible to predict an optimum catalyst loading from radiation absorption rate calculations alone. Nonetheless, the CFD approach to modeling of light intensity distribution is useful in parametric investigation for the specific photocatalytic processes.

To investigate the effect of wall reflectivity more clearly, the data in Figure 4(a) were plotted on a more sensitive scale in Figure 4(b). Clearly, for low catalyst loadings, the specularly reflecting reactor walls gave superior results. However, for higher catalyst loading (or more realistic values used in photocatalysis) the three walls gave essentially same <LVREA>. Therefore, it may be concluded that in an annular photoreactor with highly absorbing and scattering photocatalyst, the effect of reactor walls may be discarded from the reactor design and analysis. However, for optically thin mediums, the effect of wall reflectivity cannot be neglected.

CONCLUSION

A conservative variant of discrete ordinate model available in FLUENT was used to assess the effect of wall reflectivity, catalyst loading and phase function parameter on the light intensity distribution. For relatively low catalyst loadings, the wall reflectivity strongly influenced the light intensity distribution. However, for an optically thick medium, the wall reflectivity had very little or no effect. The volume-average light intensity distribution decreased rather sharply with the catalyst loading and opposite trend was obtained for LVREA. However, after

the initial sharp increase, the LVREA remained invariant of catalyst loading.

REFERENCES

- CARVALHO, M. G., and FARIAS, T. L., "Modelling of Heat Transfer in Radiating and Combustion Systems", *Transactions of IChemE, Part A*, **76**, 175 (1998).
- CASSANO, A. E., and ALFANO, O. M., "Reaction Engineering of Suspended Solid Heterogeneous Photocatalytic Reactors", *Catalysis Today*, **58**, 167-197 (2000).
- CASSANO, A. E., MARTIN, C. A., BRANDI, R. J., and ALFANO, O. M., "Photoreactor Analysis and Design: Fundamentals and Applications", *Industrial and Engineering Chemistry Research*, **34**, 2155-2201 (1995).
- CHANDRASEKHAR, S., *Radiative Transfer*, Dover, New York (1960).
- FIVELAND, W. A., "Discrete-Ordinates Solutions of the Radiative Transport Equation for Rectangular Enclosures", *Journal of Heat Transfer*, **106**, 699-706 (1984).
- PAREEK, V. K., BRUNGS, M. P., and ADESINA, A. A., "Continuous Process for Photodegradation of Industrial Bayer Liquor", *Industrial and Engineering Chemistry Research*, **40**, 5120-5125 (2001).
- PAREEK, V.K., S. J. COX, M. P. BRUNGS, B. YOUNG and ADESINA, A.A., Computational Fluid Dynamic (CFD) Simulation of a Pilot-Scale Annular Bubble Column Photocatalytic Reactor. *Chemical Engineering Science*, **58**: 959-865 (2003).
- PASQUALI, M., SANTARELLI, F., PORTER, J. F., and YUE, P.-L., "Radiative Transfer in Photocatalytic Systems", *AIChE Journal*, **42**, 532-537 (1996).
- ROMERO, R. L., ALFANO, O. M., and CASSANO, A. E., "Cylindrical Photocatalytic Reactors. Radiation Absorption and Scattering Effects Produced by Suspended Fine Particles in an Annular Space", *Industrial and Engineering Chemistry Research*, **36**, 3094-3109 (1997).
- SPADONI, G., BANDINI, E., and SANTARELLI, F., "Scattering Effects in Photosensitized Reactions", *Chemical Engineering Science*, **33**, 517-524 (1978).